Geophysical Research Letters®

Key Points:

- Fe-Mn (oxyhydr)oxide alteration combined with Mo thiolation leads to a more than 20-fold enrichment of Mo within the sulfate-methane transition zone
- Adsorption of hydrothermally derived Mo onto Fe-Mn (oxyhydr)oxide results in extremely low δ^{98}Mo values in the solid phase
- Potential postdepositional effects need to be assessed when using Mo-based proxies for paleoredox reconstruction

Correspondence to:

W. Yao,
yaowq@sustech.edu.cn

Author Contributions:

Conceptualization: Jingbo Nan, Man-Yin Tsang, Weiqi Yao
Formal analysis: Jingbo Nan, Jie Li, Male Köster, Susann Henkel, Fanyu Lin
Funding acquisition: Weiqi Yao
Investigation: Jingbo Nan, Man-Yin Tsang, Weiqi Yao
Methodology: Jingbo Nan, Jie Li, Male Köster, Susann Henkel, Fanyu Lin
Supervision: Weiqi Yao
Writing – original draft: Jingbo Nan, Weiqi Yao

Postdepositional Behavior of Molybdenum in Deep Sediments and Implications for Paleoredox Reconstruction

Jingbo Nan[1] , Man-Yin Tsang[2,3] , Jie Li[4] , Male Köster[5] , Susann Henkel[5] , Fanyu Lin[6], and Weiqi Yao[1]

[1]Department of Ocean Science and Engineering, Southern University of Science and Technology, Shenzhen, China, [2]School of Oceanography, University of Washington, Seattle, WA, USA, [3]Department of Planetology, Kobe University, Kobe, Japan, [4]State Key Laboratory of Isotope Geochemistry, Guangzhou Institute of Geochemistry, Chinese Academy of Sciences, Guangzhou, China, [5]Alfred Wegener Institute Helmholtz Centre for Polar and Marine Research, Bremerhaven, Germany, [6]Third Institute of Oceanography, Ministry of Natural Resources, Xiamen, China

Abstract Molybdenum (Mo) is a trace element sensitive to oceanic redox conditions. The fidelity of sedimentary Mo as a paleoredox proxy of coeval seawater depends on the extent of Mo remobilization during postdepositional processes. Here we present the Mo content and isotope profiles for deep sediments from the Nankai Trough, Japan. The Mo signature suggests that these sediments have experienced extensive early diagenesis and hydrothermal alteration at depth. Iron (Fe)-manganese (Mn) (oxyhydr)oxide alteration combined with Mo thiolation leads to a more than twenty-fold enrichment of Mo within the sulfate reduction zone. Hydrothermal fluids and Mo adsorption onto Fe-Mn (oxyhydr)oxides cause extremely negative Mo-isotope values at the underthrust zone. These postdepositional Mo signals might be misinterpreted as expanded anoxia in the water column. Our findings highlight the importance of constraining postdepositional effects on Mo-based proxies during paleoredox reconstruction.

Plain Language Summary Molybdenum (Mo) serves as a proxy for marine paleoredox reconstruction, offering valuable insights into how the oceanic oxygen level evolves with Earth's climate. The reliability of the Mo proxy depends on how much Mo is transferred in and out of the sediments after deposition. In this study, we investigate the Mo content and Mo-isotope composition of sediments, along with porewater geochemistry, from the International Ocean Discovery Program (IODP) Site C0023 down to 1,200 m below seafloor. We find that post-depositional remobilization of Mo leads to Mo enrichments in sulfidic intervals of the sediment column. By contrast, at the underthrust hydrothermal zone, we suggest that Mo from hydrothermal fluids is mainly adsorbed onto mineral oxides resulting in the Mo-isotope value to as low as −1.59‰. These Mo signals deviate from their primary values during deposition, but share some similarities with those derived from a range of marine redox conditions. As such, future studies need to evaluate the Mo behavior after burial before using this proxy for paleoredox reconstruction.

1. Introduction

Redox-sensitive trace elements (RSEs) such as molybdenum (Mo), uranium (U), and vanadium (V) are widely used to reconstruct marine redox changes throughout Earth's history (Dickson, 2017; Kendall et al., 2017; Tribovillard et al., 2006). RSEs in various redox states have different solubilities and/or affinities for particulates, resulting in distinct authigenic enrichment patterns (Tribovillard et al., 2006). Under oxic conditions, Mo in the dissolved form (i.e., $Mo(VI)O_4^{2-}$) can be adsorbed to iron (Fe)-manganese (Mn) (oxyhydr)oxides. Isotopically light Mo is preferentially adsorbed, leading to an equilibrium isotopic fractionation ($\Delta^{98}Mo_{solution-solid}$) of ~1–3‰ (Barling & Anbar, 2004; Goldberg et al., 2009; Wasylenki et al., 2008). Under sulfidic conditions, thiolation (sulphurization) transfers soluble $Mo(VI)O_4^{2-}$ to poorly soluble $Mo(VI)O_xS_{4-x}^{2-}$, which is further scavenged by metal-rich particles, organic matter, and/or iron sulfides (Chappaz et al., 2014; Erickson & Helz, 2000; Hlohowskyj et al., 2021; Kendall et al., 2017). When the concentration of dissolved sulfide increases at a rate that allows near-equilibrium conditions to be maintained, $Mo(VI)O_4^{2-}$ undergoes complete thiolation, being fully converted to $Mo(VI)S_4^{2-}$ at ~11 μM dissolved sulfide (Erickson & Helz, 2000). In this case, there is no isotopic fractionation of Mo between precipitates and ambient solution (Poulson Brucker et al., 2009). On the contrary, in environments of sufficiently low dissolved sulfide concentrations (<11 μM), incomplete thiolation leads to a lower Mo-isotope value (δ^{98}Mo) in precipitates compared to that in solution due to equilibrium fractionation

$(\Delta^{98}Mo_{solution-solid} = 0.5-0.9‰)$ (Hlohowskyj et al., 2021; Dickson, 2017; Kendall et al., 2017; and references therein). The Mo-isotope fractionation associated with incomplete Mo thiolation is smaller than that of adsorption of Mo onto Fe- and Mn-oxides, but for the formation of secondary Mo enrichments the thiolation process is considered to be more significant than adsorption.

While the content and isotope ratio of Mo in sediments have often been used as paleoredox proxies of coeval seawater, postdepositional processes could overprint the pristine Mo signature (Lin et al., 2022; McManus et al., 2002; Slotznick et al., 2022). For example, if depositional conditions are sulfidic with limited porewater Mo, we expect near-complete transition of porewater Mo to the solid phase during early diagenesis in shallow layers of organic-rich sediments. As a result, additional dissolved sulfide produced in deeper layers has a minor influence on the buried Mo signal due to a lack of Mo supply (Eroglu et al., 2021). However, if sediments are sulfide-lean, Mo released from reductive dissolution of Mo-bearing minerals could diffuse up/downward until drawdown into new host minerals, leading to secondary Mo enrichments and low $\delta^{98}Mo$ values in sediments (Chen et al., 2022; Eroglu et al., 2020; Reitz et al., 2007). Furthermore, when the temperature rises, late-stage diagenesis could lead to substantial alteration of both the chemical composition and texture of sediments, for example, through fluid-rock interaction (Milliken, 2003). This process, along with potential external fluids, may also alter sedimentary Mo signatures (Ardakani et al., 2016, 2020). Recent work on sediments near hydrothermal vents reports abnormally negative $\delta^{98}Mo$ values as low as $-1.7‰$ (Goto et al., 2020), but how hydrothermal processes remobilize Mo after burial is yet to be explored.

To understand postdepositional Mo behavior and the use of Mo-based proxies for paleoredox reconstruction, we investigate deep sediments from the International Ocean Discovery Program (IODP) Expedition 370 Site C0023, which have undergone extensive early diagenesis (Kars et al., 2021; Köster et al., 2021) and hydrothermal alteration (Tsang et al., 2020). By examining RSE contents and Mo-isotope ratios of bulk sediments, along with porewater trace element concentrations, we aim to reveal factors that exert the first-order control on the Mo redistribution and $\delta^{98}Mo$ composition during postdepositional processes.

2. Materials and Methods

2.1. Study Site

The IODP Site C0023 recovers drill cores down to 1,200 m below seafloor (mbsf) in the Nankai Trough, southeast of Cape Muroto, Japan (Heuer et al., 2017). Due to the location at the subduction boundary between the southwest Eurasian plate and the Philippine Sea plate, a décollement (deformational fault) between 758 and 796 mbsf separates the above and below domains (Figure 1, Figure S1 in Supporting Information S1) (Horsfield et al., 2006). The above-thrust domain includes the upper zone (250–720 mbsf) and a reversed sulfate-methane transition zone (SMTZ, centered at 730 mbsf) that likely evolved due to upward diffusion of sulfate from a "relict" (buried) sulfate pool (Köster et al., 2021). The underthrust domain is the hydrothermally altered zone (760–1120 mbsf) affected by low-temperature hydrothermal fluids (<220°C; Tsang et al., 2020) (Figure 2).

2.2. Methods

We analyze solid-phase and porewater trace element concentrations with an inductively coupled plasma mass spectrometer (ICP-MS) and solid-phase Mo-isotope ratios with a multi-collector (MC)-ICP-MS using the double-spike method. Sample collection and analytical details are given in Supporting Information S1.

3. Results

The sedimentary Mo content between 250 and 1120 mbsf is constantly low (average = 0.76 µg g^{-1}), except for the large enrichment to 19.92 µg g^{-1} at the SMTZ (Figure 2). This exceptionally high Mo content coincides with the peak of porewater sulfide concentration as well as the lowest U and V contents. Although the U and V contents are more scattered compared to Mo, all these RSEs show coupled increases at 850 and 880 mbsf at the hydrothermally altered zone. Similarly, the solid phase $\delta^{98}Mo$ is stable (average = $-0.24‰$, $n = 2$) within the upper zone, slightly decreases to $-0.80‰$ at the SMTZ, and becomes more negative within the hydrothermally altered zone with a minimum of $-1.59‰$ at 850–880 mbsf.

The porewater Mo concentration increases between 400 and 720 mbsf from <0.5 to up ~2 µM, plateaus across the SMTZ, and then decreases to 0.2 µM at 1040 mbsf within the hydrothermally altered zone (Figure 3). The
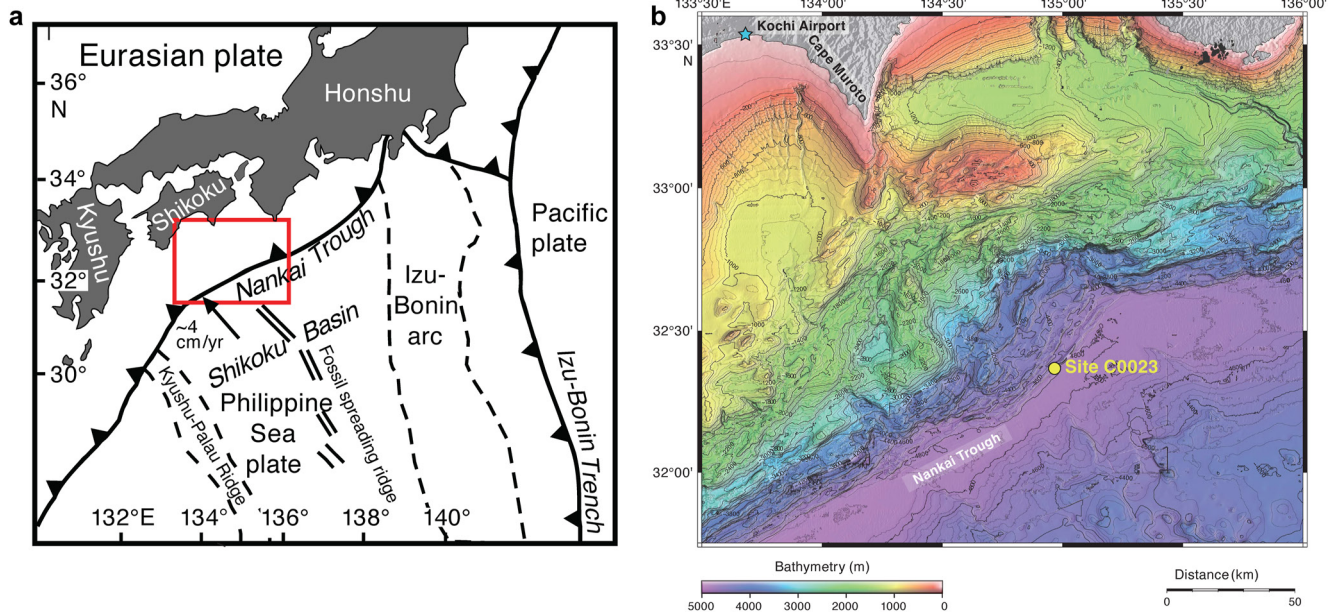
Figure 1. Geological maps of the study area. (a) Tectonic configuration of the Japanese Island system After Underwood and Guo (2018); (b) Bathymetry map of the Nankai Trough and IODP Site C0023 (Expedition 370) off Cape Muroto, Japan. After Heuer et al. (2017).

porewater U, V, and Ni concentrations remain low in the above-thrust domain (despite slightly higher V concentrations above ~400 mbsf and near the SMTZ) but show a strong variation at the hydrothermally altered zone. This pattern is similar for solid-phase RSEs and REEs (rare earth elements) (Figure 2, Figure S3 in Supporting Information S1).

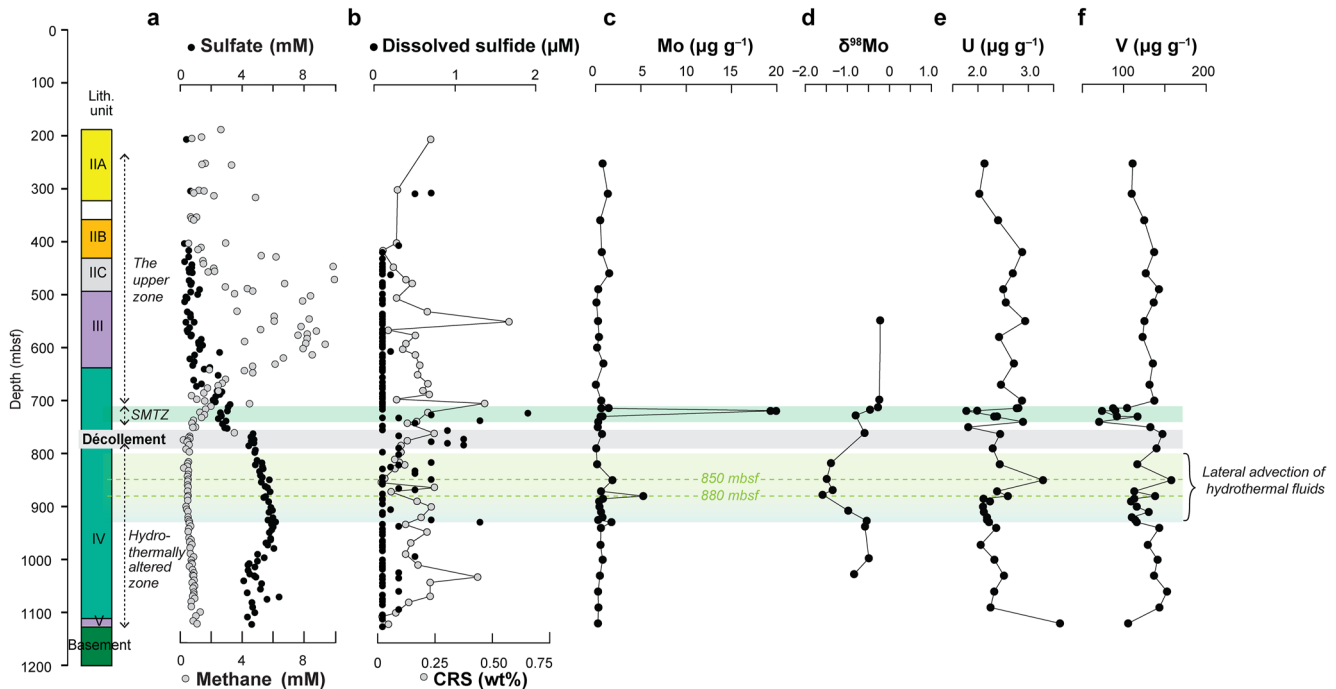**Figure 2.** Depth profiles of porewater and solid-phase geochemistry at Site C0023. (a) Porewater sulfate and methane concentrations; (b) Dissolved sulfide and pyrite (chromium reducible sulfur, CRS) content; (c, e, f) bulk solid-phase Mo, U, and V contents; (d) bulk solid-phase δ^{98}Mo. The error bar is smaller than the symbol size. Data in panels a–b are from Heuer et al., 2017; Köster et al., 2021.
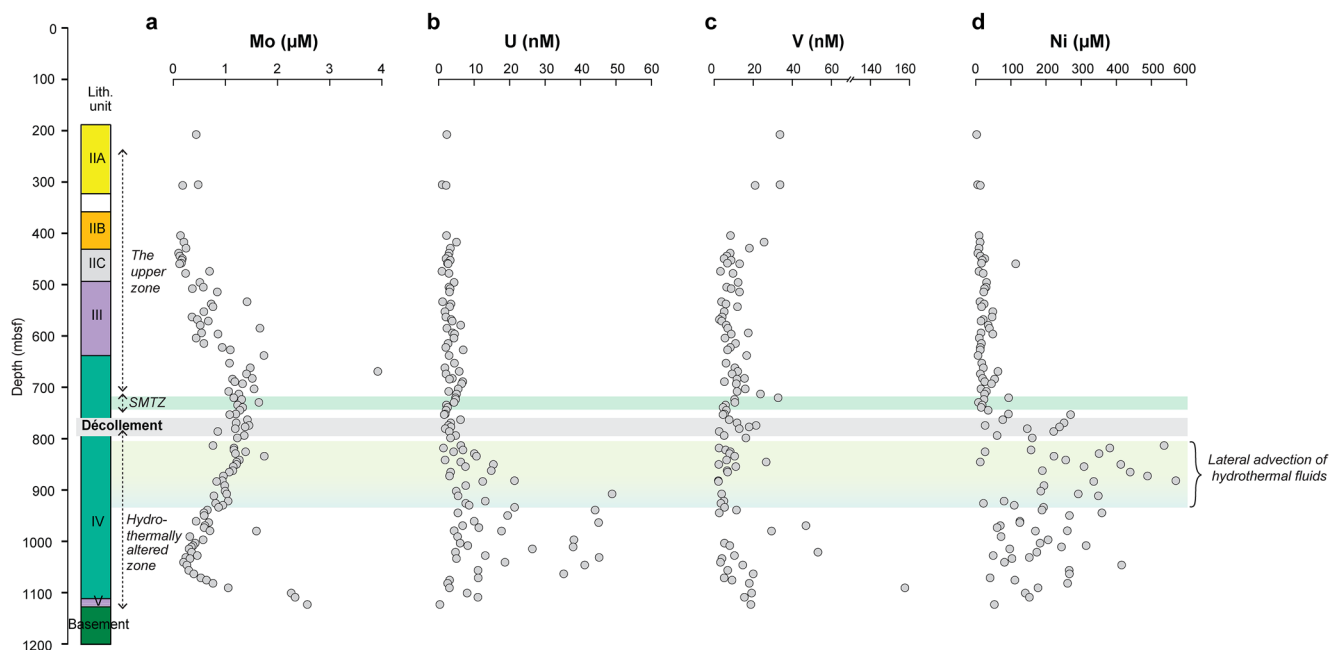
Figure 3. Depth profiles of trace element concentrations in porewater at Site C0023.

4. Discussion

4.1. Mo Behavior Across the SMTZ

The porewater sulfate and methane profiles display a reverse SMTZ sulfides (Figure 2a, Figure S4 in Supporting Information S1; Heuer et al., 2020; Kars et al., 2021; Köster et al., 2021), where iron oxides are typically transformed into Fe sulfides (e.g., Riedinger et al., 2005, 2017). During this alteration, previously adsorbed Mo is released into porewater (Figure 4). The concurrent decreases in solid-phase U, V, and REE contents within the
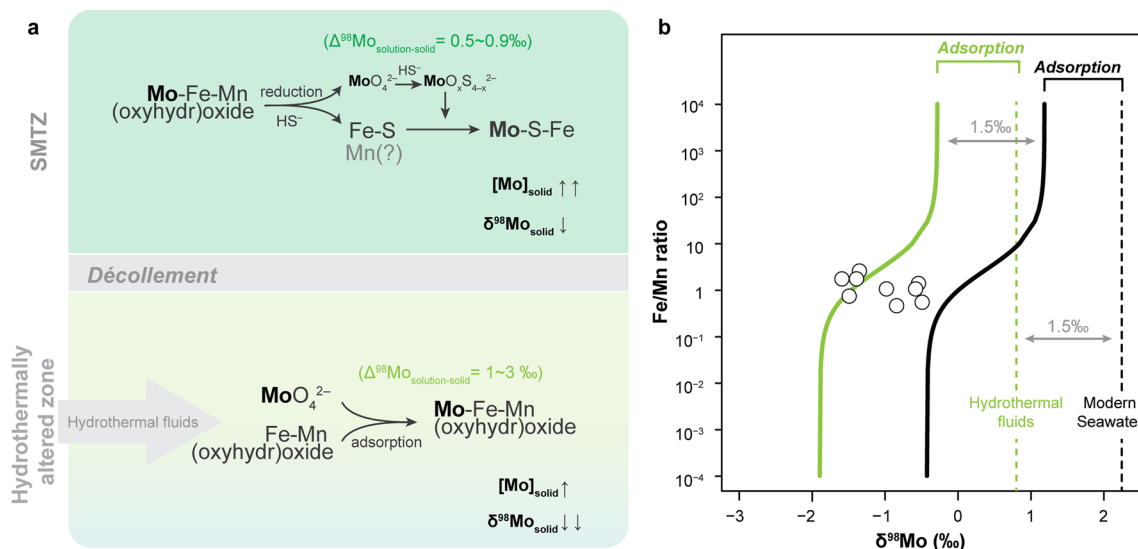
Figure 4. (a) Schematic diagram of postdepositional behavior of Mo at Site C0023. Reductive dissolution of Fe-Mn (oxyhydr)oxide and Mo thiolation control the Mo signatures at the SMTZ, while hydrothermal fluids and Mo adsorption onto Fe-Mn (oxyhydr)oxides control those at the hydrothermally altered zone. (b) The modeled sedimentary $\delta^{98}Mo$ in relation to varying Fe/Mn ratios. Fe/Mn ratios are from Heuer et al. (2017) and Köster et al. (2021) There are two source solutions: hydrothermal fluids (green dashed line) and seawater (black dashed line), providing upper and lower boundaries for the estimated solid phase $\delta^{98}Mo$ (green and black solid lines), which well covers all the observed $\delta^{98}Mo$ data from the hydrothermally altered zone. The error bar is smaller than the symbol size (open cycles).

SMTZ also indicate dissolution of Fe-Mn (oxyhydr)oxides (Figure 2, Figure S3 in Supporting Information S1), as Fe-Mn (oxyhydr)oxides have a strong capacity to adsorb U(VI), V(V), and REE(III) (Bayon et al., 2004). When the released Mo subsequently encounters dissolved sulfide produced by sulfate reduction, thiolation reduces Mo solubility, eventually resulting in a more than twenty-fold enrichment of Mo in sediments (Figure 2c). We note that the organic carbon content remains relatively stable and low (average = 0.3 wt%, Heuer et al., 2017) across this zone and was presumably also low at the time of deposition (Köster et al., 2021). Thus, scavenging of Mo by organic matter during deposition is unlikely to be the cause for the Mo enrichment.

The negative Mo-isotope excursion at the SMTZ agrees with the above finding. With the dissolved sulfide concentration being extremely low throughout the cored sediment column, and with the comparatively high Mo concentration in porewater around the SMTZ, we expect incomplete thiolation with $\Delta^{98}Mo_{\text{solution–lsolid}}$ = 0.5–0.9‰. Assuming that the $\delta^{98}Mo$ composition of sediments before burial into the deep SMTZ was similar to that at the upper zone (−0.24‰), and assuming reductive dissolution of oxides and incomplete thiolation, the resulting solid-phase $\delta^{98}Mo$ due to equilibrium fractionation would theoretically range between −0.74 and −1.14‰ (Figure 4). This is in agreement with our observation of −0.80‰ at the SMTZ (Figure 2d), and also with the reported $\delta^{98}Mo$ = −0.82‰ resulting from early diagenesis from the eastern Mediterranean (Reitz et al., 2007). Interestingly, the Mo content and $\delta^{98}Mo$ signature do not always follow the trend of pyrite at this site (i.e., paleo-SMTZ indicator). This inconsistency suggests that either the availability of paleo-porewater sulfide or Mo was limited to produce secondary Mo enrichments, or subsequent processes (e.g., the dissolution of iron sulfides) erased the paleo-Mo signal (Chappaz et al., 2014; Gregory et al., 2015).

In addition to Fe-Mn (oxyhydr)oxides dissolution, one might wonder that underthrust hydrothermal fluids and/or seawater could be potential Mo sources to the SMTZ. Hydrothermal alteration introduces fluid-bearing Mo, while seawater ions diffusing downward may carry quantitative Mo into porewater. However, according to the distinct characteristics of porewater Ni concentrations above and below the décollement, the décollement has hindered hydrothermal fluid flows from the underthrust domain (Hamada et al., 2018; Tobin & Saffer, 2009). On the other hand, similar to Eroglu et al. (2021), the influence of seawater Mo is restricted to surface layers (<10 mbsf), where sulfides at shallow depths have readily removed dissolved Mo into sediments (see Supporting Information S1). It is thus less likely to impose the observed abrupt change of Mo signals at the SMTZ. On the contrary, Fe-Mn (oxyhydr)oxide dissolution in deep sediments provides excess Mo. This process combined with Mo thiolation appears to be the primary control on the Mo signature at the SMTZ.

4.2. Hydrothermal Alteration of Mo Signatures

In the underthrust sediments, lateral advection of low-temperature hydrothermal fluids is responsible for the increases in porewater and solid-phase Mo contents. High-pressure flows result in mechanically weak areas (∼800–1050 mbsf) beneath the décollement zone (Heuer et al., 2020; Hirose et al., 2021), where Fe- and Mn-rich hydrothermal fluids intrude via lateral advection (LaRowe et al., 2020; Torres et al., 2015). Such environments favor Fe-Mn (oxyhydr)oxide formation, which explains the elevated contents of Mn and Fe oxides between 800 and 900 mbsf (Figure S3 in Supporting Information S1) (Kars et al., 2021; Torres et al., 2015). Meanwhile, hydrothermal fluids carry large amounts of trace metals (Wheat et al., 2002), which are, in turn, adsorbed onto the Fe-Mn (oxyhydr)oxides. Our results show RSEs and REEs enrichments in sediments at 850 and 880 mbsf and increasing porewater RSEs and Ni concentrations (Figure 3, Figure S4 in Supporting Information S1), suggesting the active formation of authigenic minerals associated with hydrothermal processes.

With Mo supplied by hydrothermal fluids and its adsorption onto Fe-Mn (oxyhydr)oxides, the solid phase $\delta^{98}Mo$ is shifted toward more negative values (Figure 4). To quantify the effect of Mo adsorption onto Fe-Mn (oxyhydr)oxides on $\delta^{98}Mo$, we use a simple mass balance model after Goto et al. (2020) (see details in Supporting Information S1). We conceptualize the Mo system at this zone as a box, where Mo from hydrothermal fluids constitutes the input, while Mo adsorption onto Fe-Mn (oxyhydr)oxides serves as the output. We also consider Mo-isotope fractionation ($\Delta^{98}Mo_{\text{solution–solid}}$) as a function of the Fe/Mn ratio in sediments, which ranges from 1.11‰ (Fe-oxides dominant; Goldberg et al., 2009; Goto et al., 2020) to 2.72‰ (Mn-oxides dominant; Wasylenki et al., 2008; Goto et al., 2020). Typically, the $\delta^{98}Mo$ of low-temperature hydrothermal fluids is about 0.8‰ (McManus et al., 2002). Model results suggest that the $\delta^{98}Mo$ in sediments varies between −1.92 and −0.31 ‰ (Figure 4b, green line), with lower $\delta^{98}Mo$ corresponding to lower Fe/Mn ratios. If the low-temperature hydrothermal fluids mix with some seawater via lateral advection, the source $\delta^{98}Mo$ could be higher up to 2.3‰

(i.e., the modern seawater end member; Nakagawa et al., 2012), and the resulting δ^{98}Mo in sediments is between −0.42 and 1.19‰ (Figure 4b, black line). These two scenarios provide upper and lower boundaries for the estimated δ^{98}Mo, which well covers all the observed δ^{98}Mo data from the hydrothermally altered zone. This is also in agreement with the low δ^{98}Mo of −1.7‰ found in co-precipitated Fe-Mn oxides in the modern hydrothermal setting (Goto et al., 2020).

We also note that some underthrust sediments exhibit scattered occurrences of dissolved sulfide (<11 μM), which may impact Mo through incomplete thiolation. However, Mo-isotope fractionation associated with incomplete thiolation will result in precipitates that exhibit lower Mo-isotope values compared to those found in the dissolved form with Δ^{98}Mo$_{solution–solid}$ = 0.5–0.9‰. If it were the case, hydrothermally derived Mo combined with incomplete thiolation would not explain a δ^{98}Mo value lower than −0.1‰, indicating other processes have predominantly influenced the behavior of Mo. Besides, although some intervals with relatively higher pyrite contents (Figure 2) may be indicative of paleo-SMTZs that existed prior to hydrothermal alteration (Köster et al., 2021), the associated Mo-isotope fractionation could only explain solid phase δ^{98}Mo values as low as −0.8‰ (Reitz et al., 2007 and this study). Lower values, for example, the −1.59‰ determined for the depth of 850–880 mbsf, must derive from hydrothermal alteration. We suggest that adsorption of hydrothermally derived Mo onto Fe-Mn (oxyhydr)oxides plays a main role in Mo behavior at this zone.

4.3. Challenges and Future Perspectives of Using Sedimentary Mo as a Paleoredox Proxy

The challenges of using sedimentary Mo as a paleoredox proxy stem from the difficulty in discerning postdepositional Mo enrichment processes in bulk sediments, particularly for ancient rock samples where porewater data are not available. In this study, we combine the solid-phase geochemistry and porewater data to recognize postdepositional alteration of bulk Mo signatures which offers new insights into how the modified Mo signatures could complicate the interpretation of paleoredox conditions. Specifically, the Mo enrichment at the upper zone is small and shares similarities with that in oxic marine environments, indicating a minor diagenetic impact on Mo. However, the Mo enrichment at the SMTZ and the hydrothermally altered zone increases, mimicking the pattern from oxic to reducing environments where sediments are more enriched in Mo (see Supporting Information S1 and Figure S5). Furthermore, the δ^{98}Mo value shifts toward more negative at the SMTZ and the hydrothermally altered zone compared to the upper zone (Figure S5 in Supporting Information S1). Previous studies on the early Cambrian black shales in South China have attributed the untypically low δ^{98}Mo to a more stratified ocean at continental margin settings, where the Fe-Mn (oxyhydr)oxides shuttle at shallow water depth preferentially releases isotopically depleted Mo to weakly euxinic bottom water and results in the δ^{98}Mo lower than −1.5‰ (e.g., Ostrander et al., 2019; Qin et al., 2022). However, the early Cambrian hydrothermal exhalative ore layers are present around those areas (Derkowski et al., 2013; Steiner et al., 2001), implying potential impacts from hydrothermal fluids and the associated alteration. If it is the case, hydrothermal alteration could provide an additional explanation for the extremely low δ^{98}Mo signature. That said, without considering such an effect, the extent of oceanic euxinia could be overestimated.

Drawing from our findings, comprehensive analyses of RSEs beyond Mo (e.g., U, V) are required for assessing postdepositional alteration of Mo signatures. It will be critical to identify the influence of Mo sources and sequestration pathways on Mo signatures after burial especially for the different Mo speciation. With the development of micrometer- to nanometer-scale molecular geochemical techniques, such as secondary ion mass spectrometry (SIMS), X-ray spectroscopy, identification of Mo speciation, oxidation states and phase associations in sediments becomes feasible (Slotznick et al., 2022; Tessin et al., 2019; Wagner et al., 2017). In addition, laser ablation multi-collector inductively coupled plasma mass spectrometry (LA-MC-ICPMS) has set a new benchmark for the acquisition of accurate and precise non-traditional isotopes (e.g., Fe, Mg) at the micrometer scale (Sio et al., 2013; Zhang & Hu, 2020). Thus, it may soon be possible to analyze Mo isotopes of various Mo speciation. These analytical tools offer unparalleled insights into the mechanisms of Mo enrichment and the associated isotopic fractionation, enhancing our ability to reconstruct paleoredox conditions.

5. Conclusion

Our findings suggest that postdepositional processes, including early diagenesis and hydrothermal alteration, cause Mo remobilization in deep sediments, in which different Mo sources and redox conditions play a crucial

role. Specifically, reductive dissolution of Fe-Mn (oxyhydr)oxides and the availability of dissolved sulfide control the Mo signature at the SMTZ. Notably, while the dissolved sulfide concentration is lower than the threshold of complete thiolation (11 μM), the increase in sulfide concentration primarily drives the significant Mo enrichment with small isotope fractionation. Compared to the reducing condition, the Mo content and extremely low δ^{98}Mo in hydrothermally altered sediments are likely a result of Mo adsorption onto Fe-Mn (oxyhydr)oxides. Therefore, future studies must exercise caution when using Mo-based proxies for paleoredox reconstruction. Systematic assessments of RSEs other than Mo (e.g., U, V) and micrometer- to nanometer-scale molecular geochemistry could be helpful tools to identify potential postdepositional effects and to better interpret marine paleoredox states.

Conflict of Interest

The authors declare no conflicts of interest relevant to this study.

Data Availability Statement

Additional data and figures relevant for this study are provided in Supporting Information S1. Solid-phase trace element contents, Mo isotopes, and porewater trace element concentrations are available at Nan et al. (2023).

References

Ardakani, O. H., Chappaz, A., Sanei, H., & Mayer, B. (2016). Effect of thermal maturity on remobilization of molybdenum in black shales. *Earth and Planetary Science Letters*, *449*, 311–320. https://doi.org/10.1016/j.epsl.2016.06.004

Ardakani, O. H., Hlohowskyj, S. R., Chappaz, A., Sanei, H., Liseroudi, M. H., & Wood, J. M. (2020). Molybdenum speciation tracking hydrocarbon migration in fine-grained sedimentary rocks. *Geochimica et Cosmochimica Acta*, *283*, 136–148. https://doi.org/10.1016/j.gca.2020.06.006

Barling, J., & Anbar, A. D. (2004). Molybdenum isotope fractionation during adsorption by manganese oxides. *Earth and Planetary Science Letters*, *217*(3–4), 315–329. https://doi.org/10.1016/S0012-821X(03)00608-3

Bayon, G., German, C. R., Burton, K. W., Nesbitt, R. W., & Rogers, N. (2004). Sedimentary Fe-Mn oxyhydroxides as paleoceanographic archives and the role of Aeolian flux in regulating oceanic dissolved REE. *Earth and Planetary Science Letters*, *224*(3–4), 477–492. https://doi.org/10.1016/j.epsl.2004.05.033

Chappaz, A., Lyons, T. W., Gregory, D. D., Reinhard, C. T., Gill, B. C., Li, C., & Large, R. R. (2014). Does pyrite act as an important host for molybdenum in modern and ancient euxinic sediments? *Geochimica et Cosmochimica Acta*, *126*, 112–122. https://doi.org/10.1016/j.gca.2013.10.028

Chen, S., Peng, X.-T., Li, J., Lin, Z., Li, H.-Y., Wei, G.-J., et al. (2022). Extremely light molybdenum isotope signature of sediments in the Mariana Trench. *Chemical Geology*, *605*, 120959. https://doi.org/10.1016/j.chemgeo.2022.120959

Derkowski, A., Bristow, T. F., Wampler, J. M., Środoń, J., Marynowski, L., Elliott, W. C., & Chamberlain, C. P. (2013). Hydrothermal alteration of the Ediacaran Doushantuo formation in the Yangtze Gorges area (South China). *Geochimica et Cosmochimica Acta*, *107*, 279–298. https://doi.org/10.1016/j.gca.2013.01.015

Dickson, A. J. (2017). A molybdenum-isotope perspective on Phanerozoic deoxygenation events. *Nature Geoscience*, *10*(10), 721–726. https://doi.org/10.1038/NGEO3028

Erickson, B. E., & Helz, G. R. (2000). Molybdenum(VI) speciation in sulfidic waters: Stability and lability of thiomolybdates. *Geochimica et Cosmochimica Acta*, *64*(7), 1149–1158. https://doi.org/10.1016/S0016-7037(99)00423-8

Eroglu, S., Scholz, F., Frank, M., & Siebert, C. (2020). Influence of particulate versus diffusive molybdenum supply mechanisms on the molybdenum isotope composition of continental margin sediments. *Geochimica et Cosmochimica Acta*, *273*, 51–69. https://doi.org/10.1016/j.gca.2020.01.009

Eroglu, S., Scholz, F., Salvatteci, R., Siebert, C., Schneider, R., & Frank, M. (2021). The impact of postdepositional alteration on iron- and molybdenum-based redox proxies. *Geology*, *49*(12), 1411–1415. https://doi.org/10.1130/G49291.1

Goldberg, T., Archer, C., Vance, D., & Poulton, S. W. (2009). Mo isotope fractionation during adsorption to Fe (oxyhydr)oxides. *Geochimica et Cosmochimica Acta*, *73*(21), 6502–6516. https://doi.org/10.1016/j.gca.2009.08.004

Goto, K. T., Sekine, Y., Shimoda, G., Hein, J. R., Aoki, S., Ishikawa, A., et al. (2020). A framework for understanding Mo isotope records of Archean and Paleoproterozoic Fe- and Mn-rich sedimentary rocks: Insights from modern marine hydrothermal Fe-Mn oxides. *Geochimica et Cosmochimica Acta*, *280*, 221–236. https://doi.org/10.1016/j.gca.2020.04.017

Gregory, D. D., Large, R. R., Halpin, J. A., Baturina, E. L., Lyons, T. W., Wu, S., et al. (2015). Trace element content of sedimentary pyrite in black shales. *Economic Geology*, *110*(6), 1389–1410. https://doi.org/10.2113/econgeo.110.6.1389

Hamada, Y., Hirose, T., Ijiri, A., Yamada, Y., Sanada, Y., Saito, S., et al. (2018). In-situ mechanical weakness of subducting sediments beneath a plate boundary décollement in the Nankai Trough. *Progress in Earth and Planetary Science*, *5*(1), 70. https://doi.org/10.1186/s40645-018-0228-z

Heuer, V. B., Inagaki, F., Morono, Y., Kubo, Y., Maeda, L., Bowden, S., et al. (2017). Site C0023. https://doi.org/10.14379/iodp.proc.370.103.2017

Heuer, V. B., Inagaki, F., Morono, Y., Kubo, Y., Spivack, A. J., Viehweger, B., et al. (2020). Temperature limits to deep subseafloor life in the Nankai Trough subduction zone. *Science*, *370*(6521), 1230–1234. https://doi.org/10.1126/science.abd7934

Hirose, T., Hamada, Y., Tanikawa, W., Kamiya, N., Yamamoto, Y., Tsuji, T., et al. (2021). High fluid-pressure patches beneath the décollement: A potential source of slow earthquakes in the Nankai trough off cape Muroto. *Journal of Geophysical Research: Solid Earth*, *126*(6), e2021JB021831. https://doi.org/10.1029/2021JB021831

Hlohowskyj, S. R., Chen, X., Romaniello, S. J., Vorlicek, T. P., Anbar, A. D., Lyons, T. W., & Chappaz, A. (2021). Quantifying molybdenum isotopic speciation in sulfidic water: Implications for the paleoredox proxy. *ACS Earth and Space Chemistry*, *5*(10), 2891–2899. https://doi.org/10.1021/acsearthspacechem.1c00247

Horsfield, B., Schenk, H. J., Zink, K., Ondrak, R., Dieckmann, V., Kallmeyer, J., et al. (2006). Living microbial ecosystems within the active zone of catagenesis: Implications for feeding the deep biosphere. *Earth and Planetary Science Letters*, *246*(1–2), 55–69. https://doi.org/10.1016/j.epsl.2006.03.040

Kars, M., Köster, M., Henkel, S., Stein, R., Schubotz, F., Zhao, X., et al. (2021). Influence of early low-temperature and later high-temperature diagenesis on magnetic mineral assemblages in marine sediments from the Nankai trough. *Geochemistry, Geophysics, Geosystems*, *22*(10), e2021GC010133. https://doi.org/10.1029/2021GC010133

Kendall, B., Dahl, T. W., & Anbar, A. D. (2017). The stable isotope geochemistry of molybdenum. *Reviews in Mineralogy and Geochemistry*, *82*(1), 683–732. https://doi.org/10.2138/rmg.2017.82.16

Köster, M., Kars, M., Schubotz, F., Tsang, M. Y., Maisch, M., Kappler, A., et al. (2021). Evolution of (bio-)geochemical processes and diagenetic alteration of sediments along the tectonic migration of ocean floor in the shikoku basin off Japan. *Geochemistry, Geophysics, Geosystems*, *22*(8), e2020GC009585. https://doi.org/10.1029/2020GC009585

LaRowe, D. E., Arndt, S., Bradley, J. A., Estes, E. R., Hoarfrost, A., Lang, S. Q., et al. (2020). The fate of organic carbon in marine sediments - New insights from recent data and analysis. *Earth-Science Reviews*, *204*, 103146. https://doi.org/10.1016/j.earscirev.2020.103146

Lin, Z., Sun, X., Chen, K., Strauss, H., Klemd, R., Smrzka, D., et al. (2022). Effects of sulfate reduction processes on the trace element geochemistry of sedimentary pyrite in modern seep environments. *Geochimica et Cosmochimica Acta*, *333*, 75–94. https://doi.org/10.1016/j.gca.2022.06.026

McManus, J., Nägler, T. F., Siebert, C., Wheat, C. G., & Hammond, D. E. (2002). Oceanic molybdenum isotope fractionation: Diagenesis and hydrothermal ridge-flank alteration. *Geochemistry, Geophysics, Geosystems*, *3*(12), 1–9. https://doi.org/10.1029/2002gc000356

Milliken, K. L. (2003). Late diagenesis and mass transfer in sandstone-shale sequences. *Treatise on Geochemistry*, *7–9*, 159–190. https://doi.org/10.1016/B0-08-043751-6/07091-2

Nakagawa, Y., Takano, S., Firdaus, M. L., Norisuye, K., Hirata, T., Vance, D., & Sohrin, Y. (2012). The molybdenum isotopic composition of the modern ocean. *Geochemical Journal*, *46*(2), 131–141. https://doi.org/10.2343/geochemj.1.0158

Nan, J., Tsang, M.-Y., Li, J., Köster, M., Henkel, S., Lin, F., & Yao, W. (2023). Solid-phase trace element contents, Mo isotopes, and pore-water trace element concentrations of sediment cores from IODP Hole 370-C0023A [Dataset]. PANGAEA. https://doi.pangaea.de/10.1594/PANGAEA.958415

Ostrander, C. M., Sahoo, S. K., Kendall, B., Jiang, G., Planavsky, N. J., Lyons, T. W., et al. (2019). Multiple negative molybdenum isotope excursions in the Doushantuo Formation (South China) fingerprint complex redox-related processes in the Ediacaran Nanhua Basin. *Geochimica et Cosmochimica Acta*, *261*, 191–209. https://doi.org/10.1016/j.gca.2019.07.016

Poulson Brucker, R. L., McManus, J., Severmann, S., & Berelson, W. M. (2009). Molybdenum behavior during early diagenesis: Insights from Mo isotopes. *Geochemistry, Geophysics, Geosystems*, *10*(6), Q06010. https://doi.org/10.1029/2008GC002180

Qin, Z., Xu, D., Kendall, B., Zhang, X., Ou, Q., Wang, X., et al. (2022). Molybdenum isotope-based redox deviation driven by continental margin euxinia during the early Cambrian. *Geochimica et Cosmochimica Acta*, *325*, 152–169. https://doi.org/10.1016/j.gca.2022.03.007

Reitz, A., Wille, M., Nägler, T. F., & de Lange, G. J. (2007). Atypical Mo isotope signatures in eastern Mediterranean sediments. *Chemical Geology*, *245*(1–2), 1–8. https://doi.org/10.1016/j.chemgeo.2007.06.018

Riedinger, N., Brunner, B., Krastel, S., Arnold, G. L., Wehrmann, L. M., Formolo, M. J., et al. (2017). Sulfur cycling in an iron oxide-dominated, dynamic marine depositional system: The argentine continental margin. *Frontiers in Earth Science*, *5*. https://doi.org/10.3389/feart.2017.00033

Riedinger, N., Pfeifer, K., Kasten, S., Garming, J. F. L., Vogt, C., & Hensen, C. (2005). Diagenetic alteration of magnetic signals by anaerobic oxidation of methane related to a change in sedimentation rate. *Geochimica et Cosmochimica Acta*, *69*(16), 4117–4126. https://doi.org/10.1016/j.gca.2005.02.004

Sio, C. K. I., Dauphas, N., Teng, F. Z., Chaussidon, M., Helz, R. T., & Roskosz, M. (2013). Discerning crystal growth from diffusion profiles in zoned olivine by in situ Mg-Fe isotopic analyses. *Geochimica et Cosmochimica Acta*, *123*, 302–321. https://doi.org/10.1016/j.gca.2013.06.008

Slotznick, S. P., Johnson, J. E., Rasmussen, B., Raub, T. D., Webb, S. M., Zi, J. W., et al. (2022). Reexamination of 2.5-Ga "whiff" of oxygen interval points to anoxic ocean before GOE. *Science Advances*, *8*(1). https://doi.org/10.1126/sciadv.abj7190

Steiner, M., Wallis, E., Erdtmann, B. D., Zhao, Y., & Yang, R. (2001). Submarine-hydrothermal exhalative ore layers in black shales from South China and associated fossils - Insights into a Lower Cambrian facies and bio-evolution. *Palaeogeography, Palaeoclimatology, Palaeoecology*, *169*(3–4), 165–191. https://doi.org/10.1016/S0031-0182(01)00208-5

Tessin, A., Chappaz, A., Hendy, I., & Sheldon, N. (2019). Molybdenum speciation as a paleo-redox proxy: A case study from late cretaceous western interior seaway black shales. *Geology*, *47*(1), 59–62. https://doi.org/10.1130/G45785.1

Tobin, H. J., & Saffer, D. M. (2009). Elevated fluid pressure and extreme mechanical weakness of a plate boundary thrust, Nankai Trough subduction zone. *Geology*, *37*(8), 679–682. https://doi.org/10.1130/G25752A.1

Torres, M. E., Cox, T., Hong, W. L., Mcmanus, J., Sample, J. C., Destrigneville, C., et al. (2015). Crustal fluid and ash alteration impacts on the biosphere of Shikoku Basin sediments, Nankai Trough, Japan. *Geobiology*, *13*(6), 562–580. https://doi.org/10.1111/gbi.12146

Tribovillard, N., Algeo, T. J., Lyons, T., & Riboulleau, A. (2006). Trace metals as paleoredox and paleoproductivity proxies: An update. *Chemical Geology*, *232*(1–2), 12–32. https://doi.org/10.1016/j.chemgeo.2006.02.012

Tsang, M. Y., Bowden, S. A., Wang, Z., Mohammed, A., Tonai, S., Muirhead, D., et al. (2020). Hot fluids, burial metamorphism and thermal histories in the underthrust sediments at IODP 370 site C0023, Nankai Accretionary Complex. *Marine and Petroleum Geology*, *112*, 104080. https://doi.org/10.1016/j.marpetgeo.2019.104080

Underwood, M. B., & Guo, J. (2018). Clay-mineral assemblages across the Nankai-Shikoku subduction system, offshore Japan: A synthesis of results from the NanTroSEIZE project. *Geosphere*, *14*(5), 2009–2043. https://doi.org/10.1130/GES01626.1

Wagner, M., Chappaz, A., & Lyons, T. W. (2017). Molybdenum speciation and burial pathway in weakly sulfidic environments: Insights from XAFS. *Geochimica et Cosmochimica Acta*, *206*, 18–29. https://doi.org/10.1016/j.gca.2017.02.018

Wasylenki, L. E., Rolfe, B. A., Weeks, C. L., Spiro, T. G., & Anbar, A. D. (2008). Experimental investigation of the effects of temperature and ionic strength on Mo isotope fractionation during adsorption to manganese oxides. *Geochimica et Cosmochimica Acta*, *72*(24), 5997–6005. https://doi.org/10.1016/j.gca.2008.08.027

Wheat, C. G., Mottl, M. J., & Rudnicki, M. (2002). Trace element and REE composition of a low-temperature ridge-flank hydrothermal spring. *Geochimica et Cosmochimica Acta*, *66*(21), 3693–3705. https://doi.org/10.1016/S0016-7037(02)00894-3

Zhang, W., & Hu, Z. (2020). A critical review of isotopic fractionation and interference correction methods for isotope ratio measurements by laser ablation multi-collector inductively coupled plasma mass spectrometry. *Spectrochimica Acta - Part B Atomic Spectroscopy*, *171*, 105929. https://doi.org/10.1016/j.sab.2020.105929

References From the Supporting Information

Bennett, W. W., & Canfield, D. E. (2020). Redox-sensitive trace metals as paleoredox proxies: A review and analysis of data from modern sediments. *Earth-Science Reviews*, *204*, 103175. https://doi.org/10.1016/j.earscirev.2020.103175

DeMets, C., Gordon, R. G., & Argus, D. F. (2010). Geologically current plate motions. *Geophysical Journal International*, *181*(1), 1–80. https://doi.org/10.1111/j.1365-246X.2009.04491.x

Eggins, S. M., Woodhead, J. D., Kinsley, L. P. J., Mortimer, G. E., Sylvester, P., McCulloch, M. T., et al. (1997). A simple method for the precise determination of ≥ 40 trace elements in geological samples by ICPMS using enriched isotope internal standardisation. *Chemical Geology*, *134*(4), 311–326. https://doi.org/10.1016/S0009-2541(96)00100-3

Hlohowskyj, S. R., Chappaz, A., & Dickson, A. J. (2021). Molybdenum as a paleoredox proxy. https://doi.org/10.1017/9781108993777

Inagaki, F., Kinoshita, M., Ijiri, A., Akiyama, K., Heuer, V., Homola, K., et al. (2018). JAMSTEC KR18-04 cruise report: Recovery of 1.5 years-temperature observatory data and shallow piston-core sediments from IODP Site C0023.

Li, J., Liang, X. R., Zhong, L. F., Wang, X. C., Ren, Z. Y., Sun, S. L., et al. (2014). Measurement of the isotopic composition of molybdenum in geological samples by MC-ICP-MS using a novel chromatographic extraction technique. *Geostandards and Geoanalytical Research*, *38*(3), 345–354. https://doi.org/10.1111/j.1751-908X.2013.00279.x

Moore, G. F., Taira, A., Klaus, A., Kuramoto, S., Shipley, T. H., Alex, C. M., et al. (2001). *Proceedings of the ocean drilling program, initial reports* (Vol. 190). Ocean Drilling Program.

Nägler, T. F., Anbar, A. D., Archer, C., Goldberg, T., Gordon, G. W., Greber, N. D., et al. (2014). Proposal for an international molybdenum isotope measurement standard and data representation. *Geostandards and Geoanalytical Research*, *38*(2), 149–151. https://doi.org/10.1111/j.1751-908X.2013.00275.x

Seno, T., Stein, S., & Gripp, A. E. (1993). A model for the motion of the Philippine Sea plate consistent with NUVEL-1 and geological data. *Journal of Geophysical Research*, *98*(B10), 17941–17948. https://doi.org/10.1029/93JB00782

Taylor, S. R., & McLennan, S. M. (1981). The composition and evolution of the continental crust: Rare earth element evidence from sedimentary rocks. *Philosophical Transactions of the Royal Society of London. Series A, Mathematical and Physical Sciences*, *301*(1461), 381–399. https://doi.org/10.1098/rsta.1981.0119

Zhao, P. P., Li, J., Zhang, L., Wang, Z. B., Kong, D. X., Ma, J. L., et al. (2016). Molybdenum mass fractions and isotopic compositions of international geological reference materials. *Geostandards and Geoanalytical Research*, *40*(2), 217–226. https://doi.org/10.1111/j.1751-908X.2015.00373.x